ORIGINAL ARTICLE

Multidetector CT of the Nasal Cavity and Paranasal Sinuses Variations in 73 Patients

Igor Djorić[1] · Aleksandar Trivić[2] · Mina Barna[3] · Ivan Milić[4] · Branka Marković[5] · Svetlana Valjarević[6] · Slobodan Marinković[7]

Abstract Detailed knowledge of the anatomy of the nasal cavity and paranasal sinuses is very important in the diagnosis of pathological processes, planning of endoscopic surgery, and radiologic guiding techniques during certain operations. Observational study. Clinic of Neurosurgery, Institute and Department of Anatomy and Pathology, Clinic and Department for Otorhinolaryngology and Maxillofacial Surgery, Faculty of Medicine. Two heads with brains were serially cut in the axial and coronal planes. 73 individuals, who were enrolled among 1848 patients, underwent examination by multidetector computerized tomography. A nasal septal deviation was seen in 65.8%, and septal pneumatization in 11%. Superior concha pneumatization was observed in 1.4% of patients, middle concha bullosa in 30.2%, and its hypoplasia in 1.4%. The lamina papyracea dehiscence was also present in 1.4%. The uncinate process was absent in 1.4%, and it was pneumatized in 4.2%. Agger nasi cells were noticed in 34.3%, and

✉ Slobodan Marinković
  slobodan.marinkovic@med.bg.ac.rs

  Igor Djorić
  igidren@gmail.com

  Aleksandar Trivić
  drcole71.at@gmail.com

  Mina Barna
  mina.barna@gmail.com

  Ivan Milić
  drivanmilic@gmail.com

  Branka Marković
  drmarkovicbranka@gmail.com

  Svetlana Valjarević
  cecamilosevic@gmail.com

[1] Faculty of Medicine, Clinic of Neurosurgery, Clinical Center of Serbia, Institute of Radiology, University of Belgrade, Dr. Kosta Todorović 4, 11000 Belgrade, Serbia

[2] Faculty of Medicine, Clinic for Otorhinolaryngology and Maxillofacial Surgery, Clinical Center of Serbia, University of Belgrade, Pasterova 2, 11000 Belgrade, Serbia

[3] Faculty of Medicine, Institute of Pathology, University of Belgrade, Dr. Subotić 1, 11000 Belgrade, Serbia

[4] Faculty of Medicine, Clinic of Neurosurgery, Clinical Center of Serbia, University of Belgrade, Dr. Kosta Todorović 4, 11000 Belgrade, Serbia

[5] Department of Anatomy, Faculty of Sports and Physical Education, University of Belgrade, Blagoja Parovica 156, 11000 Belgrade, Serbia

[6] Department of Otorhinolaryngology With Maxillofacial Pathology, Faculty of Medicine, Clinical Hospital Center Zemun, University of Belgrade, Vukova 9, 200140 Zemun, Serbia

[7] Faculty of Medicine, Institute of Anatomy, University of Belgrade, Dr. Subotić 4/2, 11000 Belgrade, Serbia

Haller and Onodi cells in 20.7% each. The olfactory fossa was shallow in 9.7%, deep in 31.6%, and very deep in 58.9%. Absence of the frontal sinus was seen in 9.7%. The presellar type of the sphenoidal sinus was present in 11%, the sellar in 35.7%, and the postsellar in 53.5%. Hypoplasia of the maxillary sinus was revealed in 1.4%, and hyperpneumatization in 4.2%. The sinus floor was usually below the level (60.3%), at the same level (20.7%), or above the level of the nasal floor (19.2%). The bony septum within the sinus was seen in 52.1%. The presented data are of a great significance in order to avoid a misdiagnosis of the anatomic variations, to make a proper diagnosis of certain diseases, and for safe endonasal operations.

Keywords Paranasal sinuses · Rhinology · Anatomic variations · Radiology · CT

Introduction

The pneumatic nasal cavity and the paranasal sinuses, which are interconnected via certain ostia, have a complex anatomic structure with some variations, as well as important relationships with the adjacent regions of the head and the intracranial contents [1–5]. Due to that, they are a very important subject for radiologists, otorhinolaryngologists, maxillofacial, oral and reconstructive surgeons, neurosurgeons, oncologists and some other medical experts [4, 6–10]. Obviously, their anatomic features and variations are of a great clinical significance related to radiologic imaging, diagnosis and surgery [2, 4, 6–9, 11–14].

However, a classical anatomic examination of the variations is risky and not completely reliable, especially when making sections of dry skulls. It would be far better to use complete heads for serial sections, but it is extremely difficult to provide such specimens, although we managed to provide two heads for our study. Nevertheless, we decided to use mainly a multidetector computerized tomography (MDCT) in living individuals to search for anatomic features, variations and anomalies. In general, MDCT, and sometimes cone-beam CT, are the techniques of choice in both healthy individuals and patients, particularly when using algorithms for bones, and for soft tissues occasionally [9, 15–17]. Only in some cases is magnetic resonance imaging (MRI) necessary [7, 9, 11].

The aim of our study was to examine the standard MDCT anatomy of the nasal cavity and paranasal sinuses, but especially anatomic variations, anomalies and relationships, to compare certain scans with the corresponding anatomic sections, and to perform the measurements of these cavities. Virtually each variation will be documented by the corresponding CT scans. Although certain anatomic

variants revealed in our report are known to some anatomists, and many radiologists and otorhinolaryngologists, comprehensive studies on this subject are still necessary but relatively rare in the literature [3, 13, 18–22]. In addition, some exceptional variants found in our study are commonly presented only as case reports, and some others were documented very infrequently, e.g. lamina papyracea dehiscence, bilateral uncinate process agenesis, and palatine and zygomatic recessuses of the maxillary sinus [1–4, 9, 13, 18].

Materials and Methods

The anatomic specimens will be first presented, and then the examined patients and statistical analysis.

The Anatomic Specimens

We managed to get permission from the authorities of the Institute of Anatomy and Pathology for two heads to cut them off from cadavers. The vascular system of the heads with brains was washed out with isotonic saline solution, injected then with a 10% formaldehyde solution, and fixed in the same solution for three months. Thereafter, both heads were put into a deep freezer for two weeks at minus 25^0 C. One of the heads was than serially cut in the axial plane, and the other one in the coronal plane. Sections were made at every 20 mm using a high speed circular electric saw. Each slice was carefully washed out, some elements were slightly dissected, and then the axial sections were photographed from the inferior aspect, and the coronal ones from the anterior aspect. The sections were compared to the corresponding MDCT scans of our patients.

The Examined Patients

Among the 1848 individuals, studied by MDCT for various indications during 6 months, i.e. from February to July 2020, we enrolled 73 with anatomic variations of the nasal cavity and paranasal sinuses. It is obvious that patients were randomly selected, meaning that they belong to a heterogeneous group and that their variations were revealed coincidentally. Each patient had the necessary personal record, otorhinal and general examination, and corresponding biochemical analyses, in the addition to the MDCT scans of individuals in the selected group. All serial MDCT sections were analyzed in each patient.

We used for radiologic examination Siemens Somatom Definition AS 128-slice scanner (rotation time 0.5 s, pitch 0.5, slice thickness 0.6 mm, 120–140 kV interval, manual 260 mA, noise index 3). Linear measurements of certain parameters were performed in 3 planes (axial, coronal and

sagittal) using standard software installed in the MSCT equipment.

All human studies have been approved by the Ethics Committee of the Clinical Center and the University Faculty of Medicine. An informed consent had been provided from each of the 73 individuals.

Statistical Examination

The statistical analysis comprised descriptive methods, i.e. the minimum, maximum, mean value, and standard deviation (SD). All percentages were counted in the 73 patients. Analytical statistics was also used, i.e. the Student t and the Chi-Squared test. Analysis of data was made by usage of the SPSS v. 20.0 software (Chicago, Illinois). The statistical significance was noted if a counted value reached $p<0.05$.

Results

Among the 1848 examined patients, 73 (4%) were noted to have various anatomic variations, either one or more of them. Clinical data regarding the 73 patients will be first presented, followed by a short anatomic description of the nasal cavity and sinuses, along with the observed variations and anomalies, including certain measurements of these pneumatic cavities.

Clinical Analysis

The group of the 73 patients consisted of 29 males and 44 females ($p<0.001$), who averaged 59 ± 16.65 years of age, with a range from 20 to 91 years. Of them, 60.3% had arterial hypertension and 20.7% suffered from diabetes mellitus, whilst 58.9% were cigarette smokers, and 42.5% consumed alcohol.

The patients were sent for an MDCT examination due to certain symptoms and suspected diseases or disorders: headache (64.4%), tinnitus (31.5%), other auditory or visual disorders (28.8% each), vertigo or dizziness (37.0%), facial pain (22.0%), nasal obstruction or secretion (11.0% each), a previous lacunar stroke (8.4%), head trauma (17.8%), or seizures (12.4%). Obviously, some of them showed two or more symptoms or signs.

The MDCT of some patients revealed a mucosal thickening of the nasal cavity (see later Fig. 1B, D–H), as well as of the right and left ethmoidal cells (11.0% each), the frontal sinuses (5.5% vs. 8.4%), the portions of the sphenoidal sinus (13.7% vs. 19.2%), and of the right or left maxillary sinuses (34.3% vs. 35.7%) (see later Fig. 4A), including the middle (8.4% vs. 11.0%), but also the inferior conchae (57.6% vs. 58.9%) (see later Fig. 4E–G). Tumors

were diagnosed in 2.8% of the 73 patients. As regards the entire group of 1848 examined patients, some of them showed only a slight degree of septal deviation, so that they were not included into the group of the 73 selected patients.

Nasal Cavity

The nasal cavity, which is surrounded by the paranasal sinuses, is divided into two halves by the osseous and cartilaginous nasal septum. Only two variations were found here. First, a septal deviation (Fig. 1A), noticed in 65.8% of the MDCT scans, which was most often oriented to the left. In some cases, a bony spur was observed at the most prominent part of a deviation. Second, pneumatization, which occupied the upper part of the septum (Fig. 1B), was present in 11.0% of patients.

The inferior wall of the cavity represents the hard palate (Fig. 1B, C), almost without variations in our study. The superior wall separates the nasal cavity from the anterior cranial fossa (Fig. 1C). In addition to the anterior aspect of the sphenoid body, it is mainly formed by the cribriform plate, partially divided into two parts by the crista galli, and two olfactory fossae above the plates on each side (Fig. 1C), which are described in the next passage.

The lateral wall, that borders the maxillary sinus and the orbit (Fig. 1A–D), was made up of the nasal surface of the maxilla and its frontal process, the lacrimal bone, the inferior concha, the ethmoidal labyrinth and the perpendicular plate of the palatine bone. The labyrinth contains the ethmoidal cells with two attached conchae and two meatus (Fig. 1B, C), including infundibulum with several sinus ostia described in the next passages.

Ethmoidal Sinus

It mainly consists of a relatively large number of the interconnected air cells (Fig. 1B–D) usually divided into the anterior and posterior groups (Fig. 2A). The largest of them is the ethmoidal bulla, which is mainly located posterior to the uncinate process, forming with it the semilunar hiatus (hiatus semilunaris). To the medial part of the ethmoidal labyrinth, the superior and middle conchae are attached which form the superior and middle meatus, like the isolated inferior turbinate (Fig. 1B). A thin lateral part of the labyrinth, bordering the orbit, represents the lamina papyracea (Figs. 1C, D, 2A). The cribriform plate and the crista galli form the roof of the nasal cavity (Fig. 1C). All the mentioned portions can have certain anatomic variations.

A dehiscence of the lamina papyracea was revealed bilaterally in one patient (Fig. 2B). As regards the uncinate process, its agenesis was found in one patient bilaterally (Fig. 2C). In another case, a pneumatization of the right
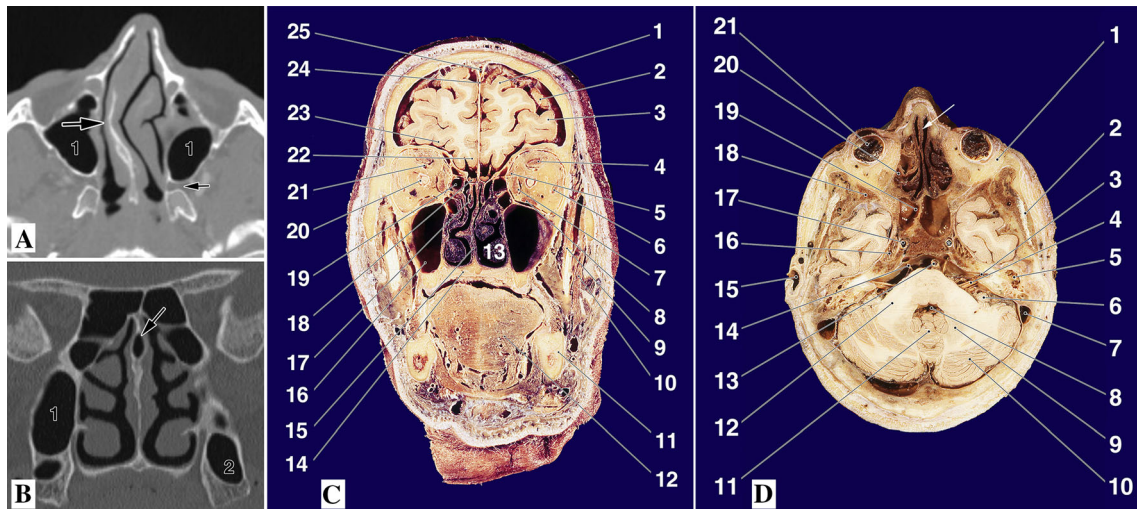
Fig. 1 A: nasal septum deviation (larger arrow), maxillary sinus (1) and pterygopalatine fossa (smaller arrow) in axial MDCT image. **B**: nasal septum pneumatization (larger arrow) with mucosal thickening in coronal MDCT image, maxillary sinus (1) and alveolar recess (2). **C**: coronal anatomic section of head to show ethmoidal and maxillary sinuses, and nasal cavity. Note superior (1), middle (2) and inferior frontal gyri (3), superior levator palpebrae and superior rectus muscles (4), superior obliquus (5), lateral rectus (6), medial rectus (7) and inferior rectus muscles (8), and temporalis (9) and masseter muscle (10), mandible (11) tongue (12), inferior concha (13), hard palate (14), nasal septum (15), right maxillary sinus (16) superior concha (17), olfactory bulb in the olfactory fossa (18), ethmoidal air cells (19), optic nerve (20), ophthalmic artery (21), straight gyrus (22), orbital gyri (23), falx cerebri (24), and superior sagittal sinus

(25). **D**: axial anatomic section of head presenting ethmoidal and sphenoidal sinuses, the latter being hypoplastic on the right side. Note periorbital tissue (1), temporalis muscle (2), internal acoustic meatus (3), facial, intermediate and vestibulocochlear nerves (4), tympanic cavity (5), flocculus (6), sigmoid sinus (7), fourth ventricle (8), dentate nucleus (9), left cerebellar hemisphere (10), vermis (11), middle cerebellar peduncle (12), basilar artery (13), abducent nerve (14), external acoustic meatus (15), trigeminal ganglion within the Meckel's cave (16), right internal carotid artery (17), and left artery (asterisk) close to the left part of the sphenoidal sinus, greater wing (18), right portion of the sphenoidal sinus with an asymmetric septum (19), ethmoidal air cells (20), eyeball (21), and nasal septum (arrow)
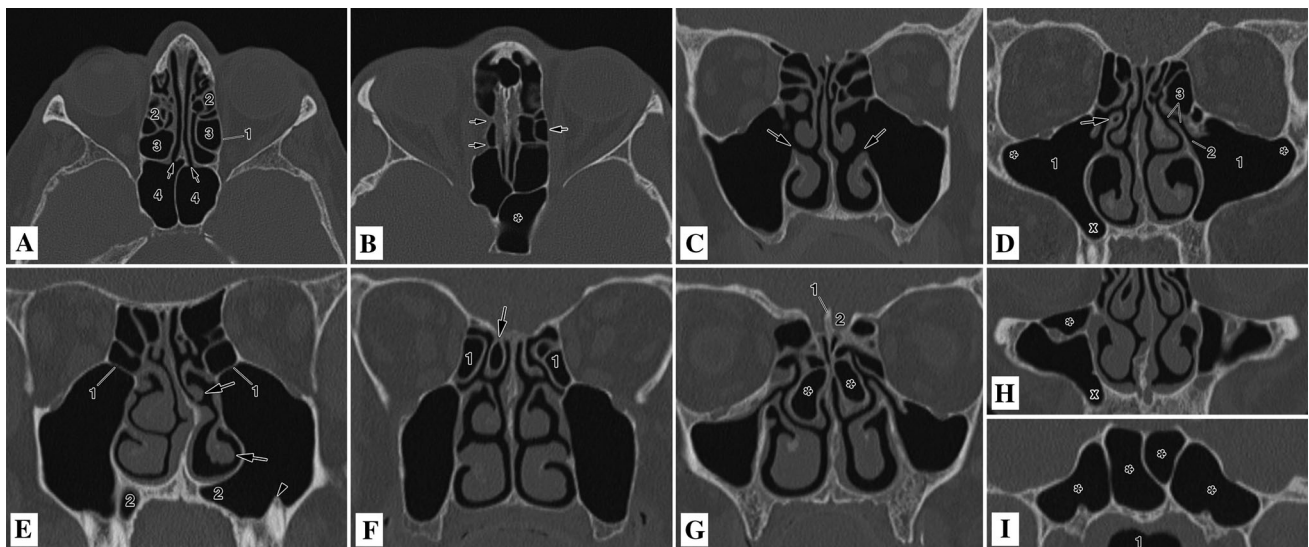

Fig. 2 Upper row showing ethmoidal variations in axial (A and B) and coronal MDCT images (C and D); **A**: normal lamina papyracea (1), anterior (2) and posterior ethmoidal cells (3), and sphenoidal sinus (4) with two ostia (arrows). **B**: bilateral lamina papyracea dehiscence (arrows) and unpaired sphenoidal sinus (*); **C**: bilateral absence of uncinate process (arrows) and its pneumatization (arrow in **D**), maxillary sinus (1) with zygomatic recess bilaterally (*), maxilllary ostium (2), semilunar hiatus and ethmoidal infundibulum (3), and alveolar recess (x). Lower row shows coronal MDCT images.

E: conchae hypoplasia (arrows), sphenomaxillary plate (1), palatine recess (2), and a molar tooth root prominence (arrowhead). **F**: superior concha bullosa (arrow) and agger nasi cells (1). **G**: bilateral middle conchae bullosae (asterisks), crista galli (1), left olfactory fossa (2), and mild hypoplasia of the maxillary sinuses. **H**: a Haller infraorbital cell (asterisk) and alveolar recess (x). **I**: Onodi cells (asterisks) above epipharynx (1)

uncinate process was seen (Fig. 2D), whilst in two others a bilateral pneumatization was present, which is 4.2% altogether (Table 1). A lateral or medial deviation of the uncinate process was occasionally observed (Table 1).

The conchae (turbinates) were normally developed in the majority of patients (Figs. 1B, C, 2C D). However, in one of them, hypoplasia was noticed (Fig. 2E). Pneumatization of the superior concha was found in 1.4% (Fig. 2F). On the other hand, the middle concha pneumatization, i.e. the concha bullosa, was noticed in 30.2%, either unilaterally or bilaterally (Fig. 2G, H) (Table 1). A paradoxical curvature of the middle concha was rarely observed

(Table 1). A secondary middle turbinate and pneumatization of the inferior concha were not found, but only hypoplasia of the latter (Fig. 2E).

Pneumatization of the ethmoidal sinus may extend anteriorly, laterally and posteriorly. In the first case, the agger nasi cells appeared, usually at the level of the lacrimal bone, i.e. along or close to the orbit and the frontal recess (Fig. 2F). These cells were present in 34.3%, most often bilaterally (Table 1). In lateral pneumatization, Haller cells were noticed in 20.7% (Table 1) below the medial part of the roof of the maxillary sinus (Fig. 2H). Posterior pneumatization was expressed as Onodi cells (Fig. 2I), with

Table 1 The anatomic variations and anomalies of the paranasal sinuses

Sinuses' portions		Anatomic variations & anomalies	Sinuses' percentages:			Patients' percentages
			Right	Left	Bilateral	
Ethmoidal	Conchae	Superior concha bullosa	1.4	0.0	0.0	1.4
	Pneumatization,	Middle concha bullosa	15.1	11.0	4.1	30.2
	Development,	Hypoplasia	0.0	1.4	0.0	1.4
	Variations	Paradoxical curvature	0.0	2.8	0.0	2.8
	Uncinate process	Agenesis	0.0	0.0	1.4	1.4
	Variations	Deviation	2.8	4.1	2.8	9.7
	Ant. Pneumatization,	Pneumatization	1.4	0.0	2.8	4.2
	lat. Pneumatization,	Agger nasi cells	4.1	5.5	24.7	34.3
	post. Pneumatization	Haller cells	11.0	8.3	1.4	20.7
	Lamina papyracea	Onodi cells	8.3	8.3	4.1	20.7
	Crista galli	Dehiscence	0.0	0.0	1.4	1.4
	Olfactory fossa	Pneumatization	/*	/	/	8.3
		Keros type I	1.4	1.4	6.9	9.7
		Keros type II	2.8	4.1	24.7	31.6
		Keros type III	5.5	6.9	46.5	58.9
Frontal	Pneumatization	Absence	2.8	5.5	1.4	9.7
	Development	Hypoplasia	0.0	1.4	0.0	1.4
Sphenoidal	Development	Agenesis	1.4	0.0	0.0	1.4
	Pneumatization ·	Hypoplasia	1.4	0.0	1.4	2.8
	Pterygoid process	Presellar type,	1.4	2.8	6.8	11.0
		sellar type,	2.8	2.8	30.1	35.7
		Postsellar type	2.8	4.1	46.6	53.5
		Hyperpneumatization	1.4	1.4	13.7	16.5
		Pneumatization	2.8	4.1	1.4	8.3
Maxillary	Development	Hypoplasia	1.4	0.0	2.8	4.2
	Pneumatization	Hyperpneumatization	1.4	1.4	1.4	4.2
	Recessuses	Frontal,	1.4	2.8	0.0	4.2
	Additional structures	zygomatic,	1.4	1.4	2.8	5.6
		Alveolar,	13.7	12.4	8.3	34.4
		Palatine	0.0	0.0	1.4	1.4
		Bony Septa	17.8	19.2	15.1	52.1
		Sphenomaxillary plate	5.5	6.9	1.4	13.8

*Unpaired structure

the same incidence, situated just in front of the sphenoidal sinus, but often in contact with its anterior wall.

The superior part of the ethmoid bone comprises the crista galli and the cribriform plates with the olfactory fossa on both sides (Figs. 1C, 2G). The crista galli was partially or completely pneumatized in 8.3% of the patients (See later Fig. 4E). The mentioned fossa, which contains the olfactory bulb (Fig. 1C), showed great variations in its depth. It was shallow in 9.7% on average, deeper in 31.6%, and very deep in 58.9% (Table 1). The straight gyrus is located just superior to the fossa and the bulb (Fig. 1C).

Frontal Sinus

This sinus is situated in the inferior and medial region of the squamous part of the frontal bone, between the external and internal tables (Fig. 3A). It is in close proximity to the nasal cavity, the orbit and intracranial contents (Fig. 1C. See later Fig. 3E–G). Two portions of the sinus were separated by a bony septum which is usually close to the midsagittal plane. The sinus measurements were presented in Table 2.

Hypoplasia of the left frontal sinus was seen in one patient (Table 1). Hyperpeumatization was not observed. Lack of pneumatization was present in 9.7% of individuals (Table 1), either unilaterally (Fig. 3A) or bilaterally (Fig. 3B). A secondary septation of the right or left sinus was not found.

As regards the drainage system, the inferior part of the sinus contains the funnel-like frontal recess on each side, previously known as the nasofrontal duct. The recess commonly opens into the anterior part of the ethmoidal infundibulum (see later Fig. 4A).

Sphenoidal Sinus

This unpaired sinus, which has a bony septum and hence two portions (Figs. 1D, 3C), is located just posterior to the
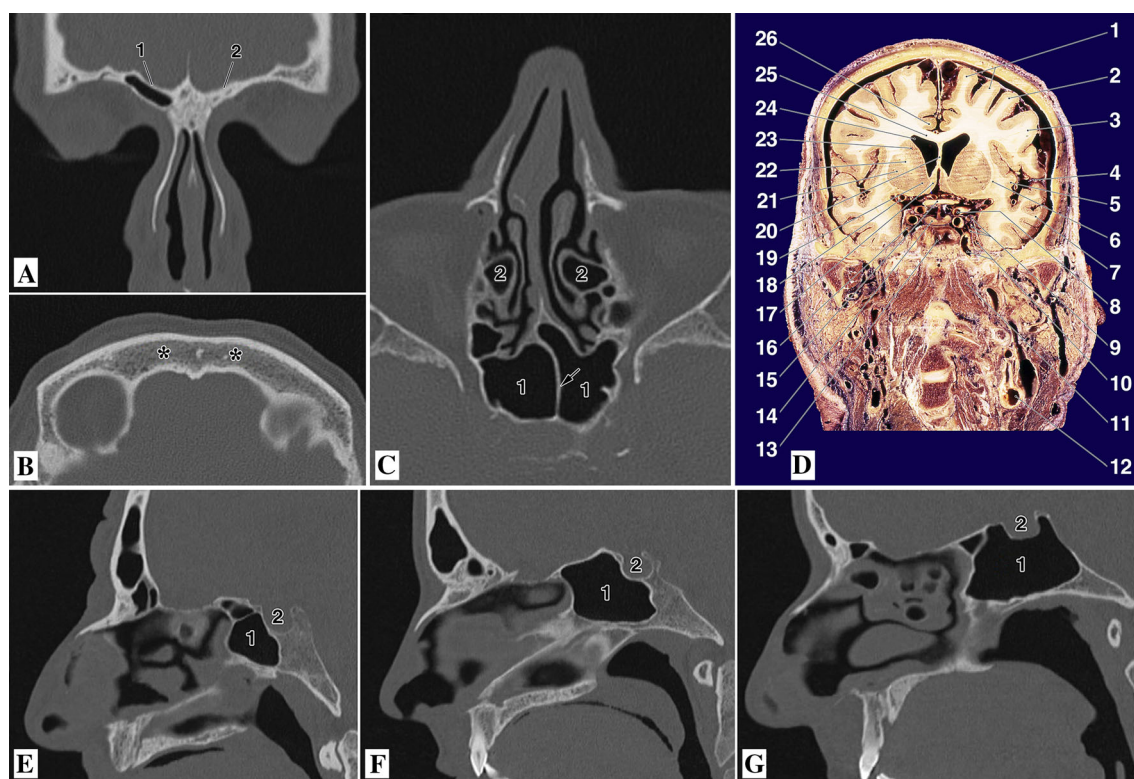

Fig. 3 Frontal and sphenoidal sinuses variations in coronal (A and D) and axial images (B and C) in upper row. **A**: right frontal sinus (1) and lack of pneumatization (2). **B**: absence of both frontal sinuses (asterisks); **C**: sphenoidal sinus (1) with its septum (arrow) and ethmoidal air cells (2); **D**: coronal anatomic section through the sphenoidal sinus. Note superior (1), middle (2) and inferior frontal gyri (3), Sylvian fissure (4), insula (5), claustrum (6), middle temporal gyrus (7), supraclinoid internal carotid artery (8), oculomotor, trochlear and abducent nerves (9), trigeminal ganglion and internal carotid artery (10), longus capitis muscle (11), common carotid artery (12), sphenoidal sinus (13), pituitary gland (14), optic chiasm (15), cavernous sinus (16), septal region (17), middle cerebral artery (18), nucleus accumbens (19), septum pellucidum (20), putamen (21), internal capsule (22), caudate nucleus (23), lateral ventricle (24), corpus callosum (25), and cingulate gyrus (26). Lower row: parasagittal MDCT sections of sphenoidal sinus (1) and hypophyseal fossa (2) showing presellar (**E**), sellar (**F**), and postsellar type (**G**)

Table 2 Measurement values of the paranasal sinuses maximum diameters in the MDCT scans

Sinuses: side, diameters		Minimum (mm)	Maximum (mm)	Mean value (mm)	Standard Deviation (SD)
Right frontal	Width	0*	94	43.62	19.51
	Depth	0	26	13.47	5.11
	Height	0	53	18.67	8.81
	Thickness**	0	9	4.23	1.86
Left frontal	Width	0	104	46.16	19.44
	Depth	0	32	15.22	5.96
	Height	0	59	21.52	9.55
	Thickness	0	9	4.14	2.00
Right sphenoidal	Width	14	77	29.14	13.14
	Depth	13	60	38.27	10.13
	Height	15	63	32.88	9.78
Left sphenoidal	Width	11	73	28.32	10.56
	Depth	14	69	37.70	12.21
	Height	15	75	33.30	10.37
Right maxillary	Width	18	115	48.47	12.52
	Depth	27	131	52.70	13.20
	Height	32	118	64.66	17.21
Left maxillary	Width	25	122	47.16	13.29
	Depth	28	137	52.64	14.35
	Height	35	119	64.21	15.97

*Absence of pneumatization
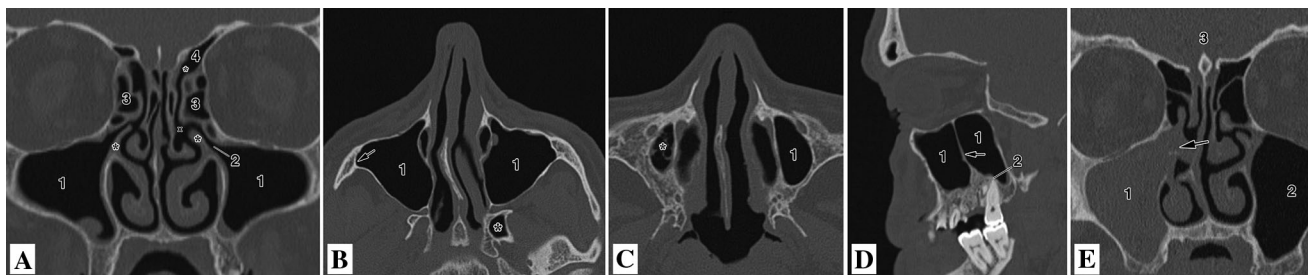
**Thickness of the anterior wall

Fig. 4 **A**: Coronal MDCT section of normal maxillary sinuses (1), maxillary ostium (2) and semilunar hiatus opening into ethmoidal infundibulum (x) close to uncinate process (larger asterisks), ethmoidal air cells (3), and frontal sinus (4) with frontal recess (smaller asterisk). **B**: axial MDCT image showing maxillary sinuses (1), right zygomatic recess (arrow) and pneumatization of left pterygoid process (asterisk); **C**: axial MDCT image of left maxillary sinus hypoplasia (asterisk), and normal left sinus (1). **D**: Parasagittal MDCT section of maxillary sinus (1) with a bony septum (arrow) and root apex (2) of a molar tooth in contact with sinus floor. **E**: coronal MDCT image presenting obstruction of right maxillary ostium (arrow) and opacification, i.e. a retention mucous cyst (1), of right maxillary sinus, and normal left maxillary sinus (2). Note pneumatization of crista galli (3)

ethmoidal cells (Figs. 2A, B, 3C) and the superior concha, and the sphenoethmoidal recess in between.

The anterior wall of the sinus, which is the posterior part of the superior wall of the nasal cavity, has a right and left draining ostium, usually lying close to the midline (Fig. 2A). The mentioned intrasinus septum occasionally shows a deviation (15.1%) (Fig. 3C), or a left or right parasagittal position, thus causing an asymmetry of the two sinus lumina, or a unilateral hypoplasia (Fig. 1D). An unpaired sinus was present in one patient (Fig. 2B) (Table 1).

The lateral wall is in relationships with the optic nerve, the superior orbital fissure and the cavernous sinus containing certain cranial nerves (the oculomotor, trochlear, abducent and ophthalmic), the internal carotid artery and the temporal lobe (Figs. 1D, 3D), and posteriorly with the petrous apex, abducent nerve, trigeminal ganglion, clivus, and the brain stem (Figs. 1D). The superior wall is just

below the sella turcica and the pituitary gland (Fig. 3D–G). The posterior wall usually merges with the basilar part of the occipital bone. The inferior surface, which anteriorly forms the superior margin of the choanae, is located just above the roof of the nasopharynx or epipharynx (Fig. 3E–G).

The sinus variations were mainly related to its pneumatization. According to the extent and relationships with the sella turcica, three main types of pneumatization can be distinguished (Table 1). First, the presellar and conchal type (Fig. 3E), situated just in front of the tuberculum sellae, which was present in 11.0% (Table 1). Second, the sellar type (Fig. 3F), below the tuberculum sellae, that was observed in 35.7% of the cases. The third or the postsellar type (Fig. 3G), lying mainly inferior and posterior to the tuberculum, had an incidence of 53.5% (Table 1).

Hyperpneumatization of the right or left portion of the sinus was usually related to the postsellar type in some patients (16.5%) (Fig. 3G). It can involve the planum (jugum) sphenoidale, the anterior clinoid process, a region of the sella turcica, including the dorsum sellae (Fig. 3G), the anterior clinoid process, and the clivus, as well as the basilar part of the occipital bone in certain patients. Pneumatization was also observed to involve the pterygoid process in 8.3% (see later Fig. 4B), either on one or both sides (Table 1).

Maxillary Sinus

The right and left sinuses (Highmore's antrum) are situated directly lateral to the nasal cavity, superior to the oral cavity, and inferior to orbit, sharing with them the same walls, as well as inferolateral to the ethmoidal air cells (Figs. 1C, 2C–H). The common medial wall contains the middle and inferior turbinates attachment, and the drainage opening, i.e. the ostium of the maxillary sinus (Figs. 2D, 4A), as well as the anterior or posterior fontanella inferiorly. The maxillary ostium terminates into the ethmoidal infundibulum via the semilunar hiatus. This opening is extremely large in the case of the uncinate process agenesis (Fig. 2C). Finally, the sinus is in close proximity to the nasolacrimal duct (Fig. 4B).

The superior wall of the sinus is the orbital floor with the infraorbital groove and canal (Figs. 1C, 2C–H), and partially with Haller cells in some patients (Fig. 2H). In the medial part of the wall, pneumatization of the frontal process was seen in 4.2% (Table 1). Between the upper part of the maxillary cavity and the ethmoidal sinuses, there was the so-called sphenomaxillary plate in (Fig. 2E) (Table 1). The anterior wall of the maxillary sinus forms the face skeleton (Figs. 1A, 4B) and contains the canalis sinuosus with the anterior superior alveolar nerve and vessels, as well as the infraorbital foramen. The posterior wall is a part of the pterygopalatine fossa (Figs. 1A, 4B), mainly containing the maxillary nerve, its branches, and twigs of the maxillary artery. The posterolateral wall forms the anterior wall of the infratemporal fossa with the pterygoid muscles, branches of the mandibular division and maxillary artery, as well as the venous plexus (Figs. 1A, 4B). The zygomatic recess (Figs. 2D, 4B) was present here in 5.6% (Table 1).

This sinus floor was below the level of the nasal cavity in 60.3% (Figs. 1C, 2C–F), at the same level in 20.7% (Fig. 2D, right), or above that level in 19.2% (Fig. 2G). In the former case, the alveolar recess was often present (Figs. 1B, 2D, H) (Table 1). On the other hand, the palatine recess was seen bilaterally only in a patient with hypoplasia of the two conchae (Fig. 2E) (Table 1). In some cases (22.0%), the root apices were in contact with the sinus floor (see later Fig. 4D) or within its lumen (Fig. 2E).

Hypoplasia of the sinus was found in 4.2% (Figs. 2G, 4C) (Table 1). Hyperpneumatization was also observed in 4.2%. In many patients (52.1%), a bony septum was almost equally present in the right and left maxillary sinus, respectively (Table 1). The septum arose from the sinus floor and extended vertically (Fig. 4D), obliquely, or rarely horizontally. In the former case, the septum occasionally reached the sinus roof (Fig. 4D).

Morphometric Examination

Measurements of the frontal, sphenoidal and maxillary sinuses were performed. The maximum width, height and depth, i.e. the anteroposterior diameter, are presented in Table 2, along with the thickness of the anterior wall of the frontal sinus.

Significant differences were observed regarding gender and certain sinuses diameters. Thus, the maximum width of both maxillary sinuses was greater in males than in females ($p = 0.003$), as was the maximum depth of the left frontal sinus ($p = 0.012$) and its maximum height ($p = 0.045$). It was the same case with all diameters of the sphenoidal sinus ($p < 0.05$).

Discussion

The nasal cavity and paranasal sinuses have been examined since the time of the ingenious Leonardo da Vinci until nowadays [1, 3, 4, 10, 18]. This is especially true in the last few decades due to the development of new imaging and surgical techniques, primarily CT examination and endoscopic surgery, which require more detailed knowledge of the anatomy of these pneumatic cavities [1, 4, 8, 9, 12, 13, 18]. This knowledge is mainly provided

by using MDCT, and rarely cone-beam CT or MRI [9, 11, 13, 16, 18, 20, 22]. MDCT imaging is necessary for making a proper diagnosis, a preoperative evaluation, following up corresponding therapeutic effects, and for creating a guiding technique during certain operations [2, 4–9, 14].

The nasal cavity and the paranasal sinuses have a complex structure and they belong to the upper airways, and partially to the olfactory system [1, 3, 23]. Along with their anatomic and functional unity, they are also involved with similar pathological processes. For example, an inflammation usually represents rhinosinusitis, and not solely rhinitis or sinusitis [2, 6, 24]. Similarly, they are often jointly affected by tumors or fractures of the face bones and the anterior or middle cranial fossa [2, 7, 13, 25].

Standard Anatomy, Variations and Anomalies

The anatomic features will be presented separately for the nasal cavity and each single paranasal sinus.

Nasal Cavity

This cavity develops embryologically from the nasal pit and sac [26]. Of its four walls in adults, we found no anomaly of the floor, but only two palatine recessuses associated with conchae hypoplasia (Fig. 2E). Other authors described certain malformations here, especially the cleft palate in some infants, as a lack of fusion of the right and left palatal shelves [26].

As regards the roof of the cavity, we noticed variations (see later) of the olfactory fossa and crista galli, similar to others [27, 28]. The choanae were normal in each individual. Choanal atresia, usually caused by a persistent oronasal membrane [26], was not present in our patients. As for the lateral wall, which borders the maxillary sinus and the orbit, it may contain some accessory ostia, especially the posterior fontanella, which is often associated with chronic sinusitis [15]. Fontanellae were observed in 10-20% of healthy individuals, but in up to 40.5% of patients with chronic sinusitis [13, 19].

Among the variants, a septal deviation was frequently found (65.8%), which is less than in some reports (83.4%) [18], probably due to the exclusion of a slight deviation in some of the 1,848 patients. The septum pneumatization was seen in 11.0%, which is more rare than in some groups of patients (22.8%) [27]. It always affected the perpendicular plate of the ethmoid bone [18]. This septal sinus can drain into the nasal cavity or the sphenoidal sinus.

Ethmoidal Sinus

This is a complex structure consisting of 3–18 small (2–3 mm^3) interconnected anterior and posterior air cells separated by basal lamella within the ethmoidal labyrinth [1, 3, 12]. The length of the labyrinth in adults is 40–50 mm, the height is 20–50 mm, the anterior width 5 mm, and the posterior width 15 mm [14].

The anterior ethmoidal cells, along with the maxillary ostium, semilunar hiatus, ethmoidal infundibulum, uncinate process and frontal recess, are named as the ostiomeatal complex or unit [19]. Some of the air cells in the middle form the ethmoidal bulla, attached to the lamina papyracea, which is rarely hypoplastic or absent, and occasionally huge in size [11, 14]. There is the semilunar hiatus between the bulla and the uncinate process [1].

The uncinate process can be attached to the medial orbital wall (85%), middle turbinate, skull base, or combined [1]. It is 3–4 mm in wide and 15–20 mm in length, but it is sometimes enlarged or elongated [14]. Its agenesis was very rare (1.4%), as well as its pneumatization [13, 14], which was found in 0.4–6.26% of the cases, compared to 4.2% in our patients (Table 1). All the mentioned variations can narrow the ethmoidal infundibulum or the semilunar hiatus [14]. The uncinate process forms the medial wall, and the lamina papyracea the lateral wall of the ethmoidal infundibulum, which is about 40 mm in length, and 5-12 mm in depth [1]. It is often the site of inflammatory polyps [9].

The lateral bony plate of the ethmoidal labyrinth, i.e. the lamina papyracea, which prevents an air outlet from the ethmoidal cells into the orbit [1], was partially absent in 1.4%. Other authors found the spontaneous dehiscence very rare [29]. In spite of this, dehiscence is clinically important because it can be the site of the orbital contents (Fig. 3) protrusion following trauma, and it can also cause a spontaneous periorbital emphysema or infections secondary to acute ethmoiditis [9].

As regards the cribriform plate, the olfactory fossa above it varied significantly in depth. Three Keros types were distinguished: a shallow one, i.e. 1–3 mm (mean, 9.7 %), deeper, that is 4–7 mm (31.6%), or very deep, i.e. 8–16 mm (58.9 %) [27]. The latter type III was the most frequent one in our study, similar to some other findings [15], whilst in certain reports type II was predominant [18, 28]. The right and left fossae were separated by the crista galli, whose pneumatization was present in 8.3%, compared with 16-29.8% in some other reports [27]. This cavity can drain into the frontal or ethmoidal sinus.

The anterior extension of the air cells represent the agger nasi cells, which were noticed in 34.3%. Their incidence is extremely variable, i.e. from 10% to over 90% of the cases [1, 13]. These cells, as well as the so-called

supra-agger frontal cells and suprabullar cells, can enter the frontal recess and even the frontal sinus, and thus compromise drainage of the sinus [30]. In this cases, pneumosinus dilatans may occur.

In the case of lateral pneumatization, Haller's cells appear inferomedial to the orbital floor (Fig. 4), i.e. just bellow the roof of the maxillary sinus [1, 11, 13, 19]. They can drain into the maxillary sinus or into the infundibulum. We observed these cells in 20.7% of patients, whilst other authors found them in 10–45% [13, 19]. The cells can compromise drainage of the maxillary sinus and cause a recurrent maxillary sinusitis.

Posterior pneumatization is related to Onodi cells, close to the sphenoidal sinus, the anterior cranial fossa, and the optic canal and nerve. We noticed them also in 20.7% (Table 1), compared to 8.0–50.8% in other reports [5, 13]. Their infection may cause the optic neuropathy, whilst iatrogenic injury of the optic nerve here may occur during sinus surgery with a consecutive blindness [13]. Finally, widening of the posterior ethmoidal cells toward the maxillary cavity (the ethmomaxillary sinus) is very infrequent (0.7–2.0%) [21].

As regards the superior concha, its pneumatization was seen in 1.4% of our patients, but between 4.9% and 50% in other reports [1, 13, 31]. The supreme concha, within the sphenoethmoidal recess, is very rare. The middle concha bullosa was present in 30.2% of our patients, which is very similar to others' data, i.e. 31.7% [13], but less than in some other articles (49%) [18]. A smaller secondary middle turbinate within the middle meatus was seen in 0.8–6.8% [1]. The inferior concha bullosa is a very rare event (0.6%) [18], as is its hypoplasia (Fig. 2E) and paradoxical curvature.

Frontal Sinus

This sinus develops from the anterior ethmoid in the 16th week of gestation [26]. Hypoplasia, noticed in one of our patients, is a very rare event [30]. A lack of pneumatization was present in 9.7% (Table 1), which is very similar to the 10.0–11.7% found by some authors [3, 30]. Hyperpneumatization, when present, may involve most of the orbital part of the frontal bone, which can explain the occurrence of meningitis or a frontal lobe abscess following a frontal sinusitis in some patients [1].

In our group, the frontal sinus measurements where somewhat larger than in other reports: the mean value of the width was 26 mm versus 24.1 mm, of the depth 18 mm versus 10.8 mm, and of the height 32 mm versus. 23.4 mm [1, 27]. As already mentioned, some sinus diameters are longer in males. The mean value of the sinus volume is about 10 cm^3 [3].

As regards the sinus septum, it is usually located close to the midline. Its pneumatization occurs infrequently. In rare cases (5.4–13.2%), the right or left sinus are separated into a medial and lateral compartment by a secondary septation [27, 32].

The frontal sinus drains via its funnel-shaped recess, i.e. the nasofrontal duct, into the ethmoidal infundibulum (Fig. 4A) or the middle meatus, but occasionally into the maxillary sinus via the ethmoidal cells [14, 33, 34]. Most often (85%), it drains medial to the uncinate process.

Sphenoidal Sinus

The sphenoidal sinus begins to develop in the 12th week of gestation from the sphenoethmoidal recess [26]. The sinus measurements (Table 2) were larger than in Hopkins' anatomic study: width 18 mm, depth 21 mm, and height 20 mm, respectively [1], as well as in a radiologic report: wide 17 mm, depth 23 mm, and height 20 mm [14]. On the other hand, the mean sinus diameter in a recent article is 30.48 mm [16], which is similar to our results. The latter authors also found a secondary sinus septation, which was not observed in our study.

As regards the pneumatization, usually three main types are distinguished: the presellar, seen in 11.0% of our patients, sellar in 35.7%, and postsellar in 53.5%. Very similar results are mentioned by some authors [18], i.e. 9.3%, 32.5% and 55%, respectively, but different in some other reports: 7%, 57% and 38% [1]. It is obvious that the sellar, and especially the postsellar types, were more frequent [16]. There is also the conchal type of the sinus, i.e. "a shallow anterior bowl with minimal pneumatization" [18], which is not related to the sella turcica [16]. This type was in combination with the presellar type in our patients.

The lack of pneumatization is very rare, i.e. less than 1%. On the other hand, hyperpneumatization sometimes involves all parts of the sphenoid bone (Fig. 15c), portions of the occipital bone, and even the atlas and axis [1, 16]. Hypopneumatization is usually related to the presellar and conchal type, whilst hypoplasia or unpaired sinus are very rare (Table 1).

Pneumatization of the pterygoid process was seen in 8.3% in our patients, compared to 13.3–16.0% reported by some authors, with a possible protrusion into the sphenoidal sinus of the pterygoid canal with the Vidian nerve, and the foramen rotundum with the maxillary division [5, 18]. There is also a protrusion of the optic canal (0.1–19%) in the case of the clinoid process pneumatization (17–23%), as well as of the carotid artery in 7% unilaterally and 16% bilaterally [13, 18].

The mean value of the sinus volume is about 10 cm^3 [9, 16]. The sinus drains via two ostia (Fig. 2A) into the sphenoethmoidal recess, and sometimes into the posterior

ethmoidal cells, or even into the nasopharynx [34]. They are round, oval or slit-like with a diameter ranging from 0.5 to 4.0 mm, and located 10–20 mm above the sinus floor [14].

The anatomic relationships of the sinus explain the possible complications of its inflammation: optic neuropathy or oculomotor nerves damage, the cavernous sinus phlebothrombosis or thrombophlebitis, the apical petrositis, and the affection of Meckel's cave with the trigeminal ganglion [13].

A close proximity of the hypophyseal fossa may explain the pituitary adenoma extension into the sphenoidal sinus, or some sinus tumors spreading into the sella turcica [7, 35]. The mentioned anatomic variations are very important during sinus surgery or a transsphenoidal pituitary approach, especially a bulging of the optic nerve or the internal carotid artery into the sinus lumen [24]. A iatrogenic injury of these two elements could result in blindness and fatal hemorrhage, respectively [21].

Maxillary Sinus

The paired, largest paranasal sinus averages about 170 cm^3 in volume [19]. It develops already in the 7th–10th week of gestation as a diverticulum of the lateral nasal wall [26]. In adults, this wall contains the maxillary ostium, 3–10 mm in diameter, and 29 mm on average above the sinus floor [19], which drains via the semilunar hiatus into the posteroinferior part of the ethmoidal infundibulum [10, 12, 34]. The latter hiatus is 1–20 mm in diameter [14]. In the case of its obstruction, a mucous retention cyst can develop, as noticed in two of the 73 patients (Fig. 4E). This drainage pathway is very large in the case with agenesis of the uncinate process, so that two large nasomaxillary cavities are formed (Fig. 2C). The accessory ostia, particularly the posterior fontanella, can be responsible for chronic maxillary sinusitis [19].

There is sometimes the sphenomaxillary plate (14–18%) between the maxillary and the ethmoidal or sphenoidal sinus (Fig. 2E) [19]. This is why some authors make a distinction between the ethmoidomaxillary and the sphenomaxillary plate [15]. Due to its presence, "the sphenoid sinus can be mistaken for posterior ethmoidal cells during the transantral ethmoidectomy" [13], which may cause a iatrogenic injury of the optic nerve or the internal carotid artery.

The sinus of our patients averaged about 48 mm in width (Table 2), which is more than in other reports, i.e. 25–35 mm [19]. It was about 64 mm in height, compared to 36–52.5 mm in other articles [1, 14, 19], and about 53 mm in depth (Table 2).

Hypoplasia, which was present in 4.2% of our patients, was observed by others in 7–10.4% [13, 15]. It can be sometimes misdiagnosed as chronic maxillary sinusitis [13]. Due to hypoplasia, orbital enlargement may appear and the consecutive enophthalmus and hypoglobus [21]. Agenesis of the sinus and atrophy of the maxilla are very rare events [19].

Hyperpneumatization was seen in 4.2% of our patients. In some cases, pneumatization of the adjacent bony structures, called recessuses, may involve the frontal, zygomatic (Figs. 2D, 4B) or palatine processes (Fig. 2E) of the maxilla (Table 1). Some of them are occasionally used for an endoscopic surgical approach to the sinus [12, 19]. The involvement of the orbital wall (the infraorbital recess) and the inferior wall (the alveolar and the palatine recess) is occasionally present.

The roof of the sinus, which is in a relationship with the orbit and the infraorbital canal, is situated about 10 mm bellow the level of the cribriform plate [1]. Due to prolapse of the mentioned canal, which occurs in 10.8%, its nerve and vessels can be injured during endoscopic surgery [19]. The posterior wall of the sinus forms the pterygopalatine fossa, whilst its posterolateral wall is the anterior border of the infratemporal fossa, where the sinus tumors or infections can spread. There is an indirect communication of the sinus with the oral cavity via the palatine foramina, with the orbit via the inferior orbital fissure or occasionally dehiscence or a thin-walled infraorbital canal, and with the middle cranial fossa by means of the foramen rotundum [1]. Due to that, an inflammation or a neoplasm from the sinus can extend into those regions [7, 19].

The sinus inferior wall, with the alveolar recess (34.4%), was below the nasal floor in 60.3%, at the same level in 20.7%, and above the level in 19.2% of our patients. This is in agreement with data from some reports, i.e. 65%, 15% and 20%, respectively [19]. The average distance between the root apices of the posterior maxillary teeth and the sinus floor is 7 mm in the region of the 2nd premolar, but only 2 mm above the roots of the 2nd molar [19]. According to some other authors, the roots of the first (92.4%) and second premolars (71.6%) penetrated into the sinus in 34.2%, and contacted the sinus floor in 36.7% of the individuals [15], which is more often than in our patients (22.2%). In any case, certain dental interventions can make communication between the oral cavity and the sinus with a consecutive development of the maxillary sinusitis [6, 17, 19].

The intrasinus septa were present in 52.1% of our patients, which is within the range of 5.5–58% reported by others [15, 18]. Usually a single septum is present, and rarely 2 or 3 of them in the same sinus, which are at least 2.5–3 mm in height. They are commonly found to originate from the region of the 1st and 2nd molars. Some septa may reach the orbital roof of the maxillary sinus (Fig. 4D).

General Remarks

Certain discrepancies among various reported data regarding anatomic variations of the maxillary and other sinuses can be explained in three ways. First, due to a great difference in the number, age and health conditions of the examined patients. Second, due to various definitions of some variations and different methods of examination, i.e. anatomic or radiologic [21]. Third, caused by certain national and ethnic differences [36]. There is a correlation between certain variants and nasal and sinuses obstruction and inflammation [13, 15, 22, 29, 30]. In any case, detailed knowledge of the variations is very important in the radiologic diagnosis of the sinus pathology, in a preparation for endonasal surgery, and in radiologic guided interventions [8, 9, 19].

Conclusions

A large number of anatomic variations and anomalies were found in the nasal cavity and paranasal sinuses in 4% of the 1,848 patients: agenesis, hypoplasia, lack of pneumatization, hyperpneumatization, dehiscence, deviation, variability of drainage systems, additional bony structures, and the corresponding relationships, including the close proximity of the posterior tooth root apices to the maxillary sinus floor, and certain cranial nerves and the internal carotid artery bulging in the sphenoidal sinus. Many of the variants can narrow or obstruct the nasal cavity or sinus ostia and thus cause acute or chronic rhinosinusitis. Some of the variants can be misinterpreted as pathological structures, and others can complicate the endoscopic sinus surgery. In any case, the anatomy of the nasal cavity and paranasal sinuses, examined by MDCT, is of a great clinical significance.

Declarations

Conflict of interest The authors have no relevant financial or non-financial interests to disclose.

Informed Consent An informed consent had been provided from each of the 73 individuals, and patients anonymity had been preserved.

Human and Animal Rights All human studies have been approved by the Ethics Committee of the Clinical Center and the University Faculty of Medicine. It has been performed in accordance with the ethical standards laid down in the 1964 Declaration of Helsinki and all subsequent revisions.

References

1. Hopkins C (2016) Nose, nasal cavity and paranasal sinuses. In: Standring S (ed) Gray's anatomy. The anatomical basis of clinical practice. Elsevier Limited, London, pp 556–570
2. Jankowski R, Nguyen DT, Poussel M, Chenuel B, Gallet P, Rumeau C (2016) Sinusology. Eur Ann Otorhinolaryngol Head Neck Dis 133:263–268
3. Krouse JH, Stachler RJ (2006) Anatomy and physiology of the paranasal sinuses. Taylor & Francis, New York, pp 55–94
4. Ogle OE, Weinstock RJ, Friedman E (2012) Surgical anatomy of the nasal cavity and paranasal sinuses. Oral Maxillofac Surg Clin North Am 24:155–166
5. Wada K, Moriyama H, Edamatsu H, Hama T, Arai C, Kojima H et al (2015) Identification of Onodi cell and new classification of sphenoid sinus for endoscopic sinus surgery. Int Forum Allergy Rhinol 5:1068–1076
6. Crovetto-Martínez R, Martin-Arregui FJ, Zabala-López-de-Maturana A, Tudela-Cabello K, Crovetto-de la Torre MA (2014) Frequency of the odontogenic maxillary sinusitis extended to the anterior ethmoid sinus and response to surgical treatment. Med Oral Patol Oral Cir Bucal 19:e409-413
7. Kawaguchi M, Kato H, Tomita H, Mizuta K, Aoki M, Hara A et al (2017) Imaging characteristics of malignant sinonasal tumors. J Clin Med 6:116
8. Kingdom TT, Orlandi RR (2004) Image-guided surgery of the sinuses: current technology and applications. Otolaryngol Clin N Am 37:381–400
9. Maroldi R, Ravanelli M, Borghesi A, Farina D (2008) Paranasal sinus imaging. Eur J Radiol 66:372–386
10. Ozcan MK, Selcuk A, Oruk V, Dere H (2008) Ethmomaxillary sinus. Eur Arch Otorhinolaryngol 265:185–188
11. Aygun N, Uzuner O, Zinreich JS (2005) Advances in imaging of the paranasal sinuses. Otolaryngol Clin N Am 38:429–437
12. Hosemann W, Grimm A (2020) Surgical anatomy of the maxillary sinus. HNO 68:555–565
13. Kantarci M, Karasen MR, Alper F, Onbas O, Okur A, Karaman A (2004) Remarkable anatomic variations in paranasal sinus region and their clinical importance. Eur J Radiol 50:296–302
14. Polavaram R, Devaiah AK, Sakai O, Shapshay SM (2004) Anatomic variants and pearls–functional endoscopic sinus surgery. Otolaryngol Clin N Am 37:221–242
15. Ata-Ali J, Diago-Vilalta JV, Melo M, Bagán L, Soldini M-C, Di-Nardo C et al (2017) What is the frequency of anatomical variations and pathological findings in maxillary sinuses among patients subjected to maxillofacial cone beam computed tomography? A systematic review. Med Oral Patol Oral Cir Bucal 22:e400–e409

16. Singh P, Hung K, Ajmera DH, Yeung AWK, von Arx T, Bornstein MB (2021) Morphometric characteristics of the sphenoid sinus and potential influencing factors: a retrospective assessment using cone beam computed tomography (CBCT). Anat Sci Int. https://doi.org/10.1007/s12565-021-00622-x

17. Gu Y, Sun C, Wu CG, Zhu Q, Leng D, Zhou Y (2018) Evaluation of the relationship between maxillary posterior teeth and the maxillary sinus floor using cone-beam computed tomography. BMC Oral Health 18:164

18. Devaraja K, Doreswamy SK, Pujary K, Ramaswamy B, Pillai S (2019) Anatomical variations of the nose and paranasal sinuses: a computed tomographic study. Indian J Otolaryngol Head Neck Surg 71:S2231–S2240

19. Whyte A, Boeddinghaus R (2019) The maxillary sinus: physiology, development and imaging anatomy. Dentomaxillofac Radiol 48:20190205

20. Kaplanoglu H, Kaplanoglu V, Dilli A, Toprak U, Hekimoğlu B (2013) An analysis of the anatomic variations of the paranasal sinuses and ethmoid roof using computed tomography. Eurasian J Med 45(2):115–125

21. Papadopoulou AM, Chrysikos D, Samolis A, Tsakotos G, Theodore Troupis T (2021) Anatomical variations of the nasal cavities and paranasal sinuses: a systematic review. Cureus 13(1):e12727

22. Qureshi MF, Usmani A (2021) A CT-Scan review of anatomical variants of sinonasal region and its correlation with symptoms of sinusitis (nasal obstruction, facial pain and rhinorrhea). Pak J Med Sci 37(1):195–200

23. Sieron HL, Sommer F, Hoffmann TK, Grossi A-S, Scheithauer MO, Stupp F et al (2020) Function and physiology of the maxillary sinus. HNO 68:566–572

24. Solari D, Cavallo LM, Cappabianca P (2014) Surgical approach to pituitary tumors. Hand Clin Neurol 124:291–301

25. Roselló EG, Granado AMQ, Garcia MA, Martí SJ, Sala GL, Beltrán B et al (2020) Facial fractures: classification and highlights for a useful report. Insights Imaging 19(11):49

26. O'Rachilly R, Müller F (2001) Human embryology & teratology, 3rd edn. Wiley-Liss. A John Wiley & Sons Inc Publication, New York, pp 285–288

27. Acar G, Cidekcibasi AE, Koplay M, Kelesoglu KS (2020) The relationship between the pneumatization patterns of the frontal sinus, crista galli and nasal septum: a tomography study. Turk Neurosurg 30:532–541

28. Babu AC, Nair MR, Kuriakose AM (2018) Olfactory fossa depth: CT analysis of 1200 patients. Indian J Radiol Imaging 28:395–400

29. Mezri S, Sayhi S (2019) Dehiscence of the lamina papyracea. Pan Afr Med J 34:77 (**Article in French**)

30. Sommer F, Hoffmann TK, Harter L, Döscher J, Kleiner S, Lindemann J et al (2019) Incidence of anatomical variations according to the International Frontal Sinus Anatomy Classification (IFAC) and their coincidence with radiological signs of opacification. Eur Arch Otorhinolaryngol 276:3139–3146

31. İla K, Yilmaz N, Öner S, Başaran E, Öner Z (2018) Evaluation of superior concha bullosa by computed tomography. Surg Radiol Anat 40:841–846

32. Comer BT, Kincaid NW, Smith NJ, Wallace JH, Kountakis SE (2013) Frontal sinus septations predict the presence of supraorbital ethmoidal cells. Laryngoscope 123:2090–2093

33. Lee D, Brody R, Har-El G (1997) Frontal sinus outflow anatomy. Am J Rhinol 11:283–285

34. Mann WJ, Tóth M, Gouveris H, Amedee RO (2011) The drainage system of the paranasal sinuses: a review with possible implications for balloon catheter dilation. J Rhinol Allergy 25:245–248

35. Ramakrishnan VR, Suh JD, Lee JY, O'Malley BW Jr, Grady MS, Palmer JN (2013) Sphenoid sinus anatomy and suprasellar extension of pituitary tumors. J Neurosurg 119:669–674

36. Mokhasanavisu VJP, Singh R, Balakrishnan R, Kadavigere R (2019) Ethnic variation of sinonasal anatomy on CT scan and volumetric analysis. Indian J Otolaryngol Head Neck Surg 71(Suppl 3):2157–2164